Accepted Manuscript

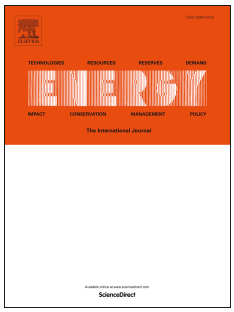

Fuel cell as an effective energy storage in reverse osmosis desalination plant powered by photovoltaic system

Hegazy Rezk, Enas Taha Sayed, Mujahed Al-Dhaifallah, M. Obaid, Abou Hashema M. El-Sayed, Mohammad Ali Abdelkareem, A.G. Olabi

PII: S0360-5442(19)30373-1

DOI: https://doi.org/10.1016/j.energy.2019.02.167

Reference: EGY 14809

To appear in: *Energy*

Received Date: 3 October 2018

Revised Date: 15 January 2019

Accepted Date: 23 February 2019

Please cite this article as: Rezk H, Sayed ET, Al-Dhaifallah M, Obaid M, El-Sayed AHM, Abdelkareem MA, Olabi AG, Fuel cell as an effective energy storage in reverse osmosis desalination plant powered by photovoltaic system, *Energy* (2019), doi: https://doi.org/10.1016/j.energy.2019.02.167.

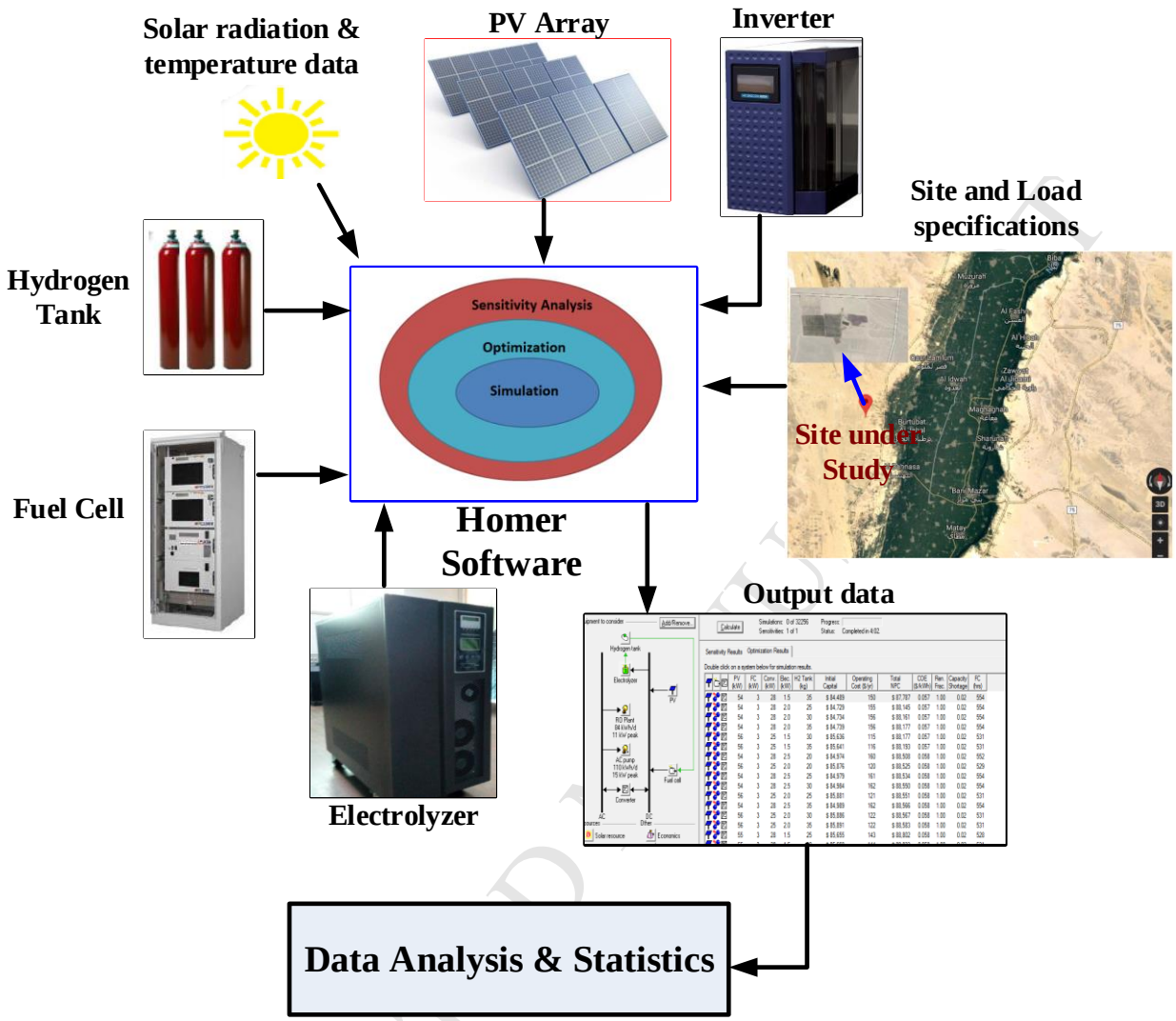

Fuel Cell as an Effective Energy Storage in Reverse Osmosis Desalination Plant Powered by Photovoltaic System

Hegazy Rezk[1, 2*], Enas Taha Sayed[3,4], Mujahed Al-Dhaifallah[5], M. Obaid[3,6], Abou Hashema M. El-Sayed[2], Mohammad Ali Abdelkareem[7,4,3], and A.G. Olabi[7,8,]**

[1]College of Engineering at Wadi Addawaser, Prince Sattam Bin Abdulaziz University, KSA
[2]Electrical Engineering Department, Faculty of Engineering, Minia University, Egypt
[3]Chemical Engineering Department, Minia University, Elminia, Egypt
[4]Center of Advanced Materials Research, Research Institute of Science and Engineering, University of Sharjah, P.O. Box 27272, Sharjah, United Arab Emirates
[5]Systems Engineering Department, King Fahd University of Petroleum and Minerals, Dhahran, 31261, KSA
[6]Global Desalination Research Center (GDRC), School of Earth Sciences and Environmental Engineering, Gwangju Institute of Science and Technology (GIST), Republic of Korea
[7]Dept. of Sustainable and Renewable Energy Engineering, University of Sharjah, P.O. Box 27272, Sharjah, UAE
[8]Mechanical Engineering and Design, Aston University, School of Engineering and Applied Science, Aston Triangle, Birmingham, B4 7ET, UK

Corresponding authors:
** A.G. Olabi;
*Hegazy Rez; Tel.: 00966547416732, Fax:00966115882000, Email hegazy.hussien@mu.edu.eg.

***Abstract*—** A hybrid renewable energy systems (HRESs) comprises of photovoltaic (PV), and self-charging fuel cells (SCFC) is designed for securing electrical energy required to operate brackish water pumping (BWP) and reverse osmosis desalination (RO) plant of 150 m^3d^{-1} for irrigation purposes in remote areas. An optimal configuration of the proposed design is determined based on minimum cost of energy (COE) and the minimum total net present cost (NPC). Moreover, a comparison with a stand-alone diesel generation (DG) or grid extension is carried out against the optimal configuration of PV/SCFC HRES. The modeling, simulation, and techno-economic evaluation of the different proposed systems, including the PV/SCFC system are done using HOMER software. Results show that PV array (66 kW), FC (9 kW), converter (25 KW) –Electrolyzer (15 kW), Hydrogen cylinder (70 kg) are the viable economic option with a total NPC of $115,649 and $0.062 unit cost of electricity. The COE for the stand-alone DG system is 0.206 $/kWh, which is 69.90 % higher than that of the PV/SCFC system. The PV/SCFC system is cheaper than grid extension. This study opens the way for using a fuel cell as an effective method for solving the energy intermittence/storage problems of renewable energy sources.

Key words: Stand-alone hybrid system; photovoltaic cells; fuel cells; reverse osmosis desalination; energy efficiency

1. Introduction

Securing freshwater resources with minimum cost and no environmental impact is a worldwide target that needs solving. Renewable energy is an attractive alternative for water desalination plants especially in remote areas where there is no connect to the grid [1, 2]. Solar energy, wind energy, and others are promising renewable energy sources that are environmentally safe, cheap running cost, low maintenance, however, their intermittence is one of the main challenges associated with their applications. Therefore, a stand-alone hybrid energy system is considered an effective way that could be used to overcome this problem. Securing a reliable, cost-effective stand-alone renewable energy attracts the attention of several researchers [3]. Photovoltaic cells (PV) are among the most applicable renewable energy where it can secure electricity in arid areas with minimum operating and maintenance costs; however, the intermittence nature of solar energy, from day to night, and its dependence on weather conditions, cloudy or not, limits their applications for limited time periods when solar energy is available. Therefore, PV systems are usually hybrid with batteries and/or diesel generators [4]. Limitations of lead-acid batteries are; short life expectancy, high replacement cost, poor performance at low temp and high temp, air-conditioning sometimes is needed, the cost increases in a linear fashion when more backup time is needed and the environmental concerns with

used batteries. Whereas the limitations of the DG system include; frequent maintenance required, polluting, very noisy, the cost of the fuel, the cost of fuel transportation, and subject to numerous regulations [5].

Fuel cells (FCs) are electrochemical devices that are used for direct conversion of chemical energy of fuels into electricity with high efficiency. Besides high efficiency, fuel cells have several advantages such as silent, smaller in size compared to other energy conversion devices, low or no environmental impact [6], moreover, it can work on different fuels that can be obtained from renewable resources such as methanol [7], ethanol [8], formic acid [9], biogas [10, 11], syngas [12], and biochar [13]. Moreover, FCs are also used for simultaneous wastewater treatment and electricity generation, such as in urea fuel cells [14] and microbial fuel cells [15, 16]. Due to the extensive progress in renewable energy, conventional storage devices such as batteries can no longer meet these storage requirements, especially where grid connection is not available. Flow batteries demonstrated promising results in terms of high energy density and life time especially those using three electrolyte configuration [17-20]. However, their application is restricted by the high cost (in case of using precious materials) and some technical issues that need to be solved out before commercialization [21]. Therefore, innovative ways are developed to meet such high energy storage capabilities such as a water electrolyzer/FC system [22, 23]. Electrolyzer/FC was found to be the best among different storing alternatives such as pumped hydro, supercapacitors, pressurized air, battery and flywheel based on different criteria such as cost, power/energy density, environmental impact, safety, ease of integration, efficiency, and durability [23]. Simulation results showed that waste heat recovery of the fuel cell as well as using the excess hydrogen could significantly improve the efficiency of the solar/electrolyzer/FC system to 80 % higher heating values of hydrogen [24]. Using MATLAB, a cost analysis has been carried out on an RO driven by PV integrated with electrolyzer/FC as energy storage. The energy balance done in this study was made only for one day during the year, and no comparison with grid carried out [25]. An electrolyzer/FC is investigated as energy storage for PV and/or wind hybrid energy to power a water desalination plant of an average capacity of 193.6 m^3 per year in Tunisia using iterative optimization technique [26]. Results showed that the hybrid PV/wind is preferable in reducing the storage requirements by deciding the optimal capacities of the wind turbine, PV, electrolyzer, hydrogen storage and FC [26]. A hybrid PV/FC system for application to desalination is also investigated in ref. [27] where the authors calculated the size of the different components of the system. However, the calculations done in this study were not based on the exact load demand that resulted in a significant energy loss of 160 kWh. Also, the study did not include any comparison with any other energy sources. Table I shows some common hybrid energy systems used for different applications. It can be noted that the COE is varied from 0.09 $/kWh to 4.780.09 $/kWh. This encourages the authors to consider a PV/FC hybrid system as an alternative with expected lower COE, especially in arid areas.

Table I: some common different hybrid systems including the cost of energy (COE) and the country of study.

Author	Year	Configuration	Country	Load	COE, $/kWh
Ghenai and Maamar [28]	2019	PV/FC/DG	UAE	University building	0.92
Luta and Raji [29]	2019	PC/FC/supercapacitor	South Africa	Commercial facility	4.78
Das and Zaman [30]	2019	PV/DG/battery	Bangladesh	Household	0.31
Fodhil et al. [31]	2019	PV/DG/battery	Algeria	20 Households	0.37
C. Ghenai et al. [32]	2018	PV/grid	UAE	Desalination plant	0.09
C. Ghenai et al. [32]	2018	PV/DG/battery	UAE	Desalination plant	0.367
C. Ghenai et al. [33]	2018	PV/FC/grid	UAE	Residential	0.145
A. Singh [34]	2017	PV/FC/battery	India	Building	0.203
Rajbongshi et al. [35]	2017	PV/biomass/DG/battery	India	Different loads	0.145
Amutha and Rajini. [36]	2015	SPV/WES/battery/DG/FC	India	Telecom load	0.997
Khan et al. [37]	2015	PV/hydro/DG/battery	China	Island	0.142
Lau et al. [38]	2015	PV /DG/battery	Malaysia	Island	0.569
Rohani et al. [39]	2014	PV/wind/ DG /battery	UAE	Remote areas	0.2
Kusakana. [40]	2014	Hydrokinetic/ DG /battery	South Africa	Rural household	0.265
Chong Li et al. [41]	2013	wind/PV/battery	China	Household	1.045

M. Salam et al. [42]	2013	PV/battery	Oman	Lighting	0.561
Hiendro et al. [43]	2013	PV/wind/battery	Indonesia	Village	0.751
A. Hiendro et al. [44]	2013	PV/wind	Indonesia	AC load	1.06
Nandi et al. [45]	2010	Wind/PV/battery	Bangladesh	Remote area	0.47
Rehman et al. [46]	2010	PV/DG/battery	Saudi Arabia	Remote area	0.19
Lau et al. [47]	2010	PV/ DG	Malaysia	Remote area	0.275

This study shows technical and economic feasibility of applying a hybrid energy system of PV and self-charging fuel cells (SCFC), PV/SCFC to power a BWRO desalination unit for irrigation in remote areas in Egypt. A techno-economic analysis of the PV/SCFC was done using a hybrid optimization model for electric renewable (HOMER) for identifying the best configuration from an economic and environmental point of views based on NPC and COE. Additionally, a comparison with stand-alone DG system and with grid extension are carried out against the optimal configuration of PV/SCFC HRES. The study showed that the PV/SCFC as a fordable and environmental system for desalination in arid areas. Moreover, installing PV/SCFC hybrid system is much cheaper than grid extension. The breakeven grid extension distance for DG system and PV/SCFC hybrid system were found to be 41.5 km and 8.21 km, respectively.

2. Site Location & Load Profile

The site selected for this study is located in Minya city, Egypt at 28° 38′ latitude north and 30° 35′ longitude east of a flat 70 acres as can be seen in Fig.1. The site contains a well at 150 m depth with a static water level of 40 m and produces brackish water of 2500 gm/l at 120 m^3/hour. It is proposed to cultivate the land with olive that can use the available brackish water while a section of the land will be cultivated with other crops such Wheat which needs water with salinity less than 800 gm/l that is, in turn, will result in decreasing land salinity in the long term usage. The estimated amount of treated water for this portion of land is around 75 m^3/day. The estimated brackish water requirements for both olives and wheat is 350 to 500 m^3 of water in summer, and this amount decreased by 150 m^3 in winter.

The electrical power required for the pumping system is calculated using the following equation [48] ;

$$P_{pump} = \frac{2.725QH}{1000\eta} \quad (1)$$

Where; P_{pump} is the electrical power requirement for the pump (kW); H is the pumping head (m) and η is the efficiency of the pump. The power required for brackish water pumping (BWP) is found to be 110 kWh/day with 15 kW peak demand [49-51]. The variation of the daily pumping power requirements overall the year is shown in Fig. 2.

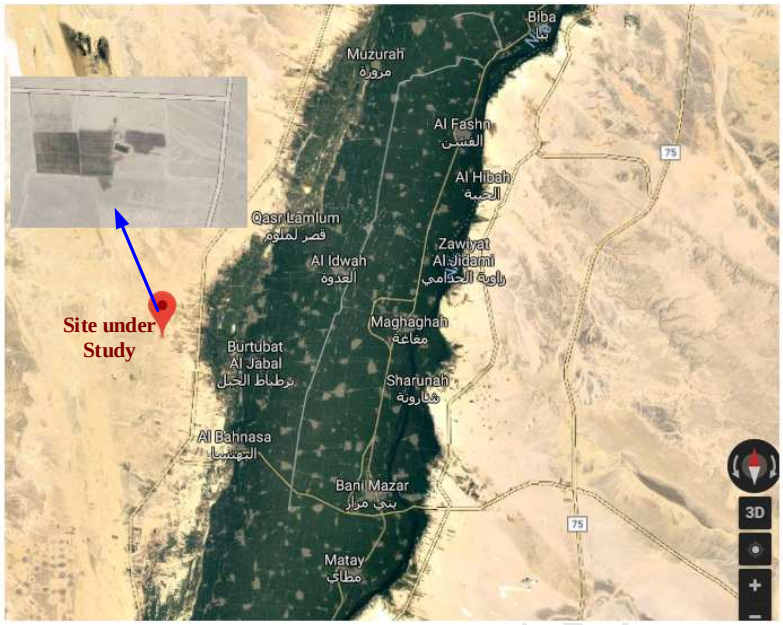

Fig. 1 Geographical location of the site under study at Alminiya city, Egypt.

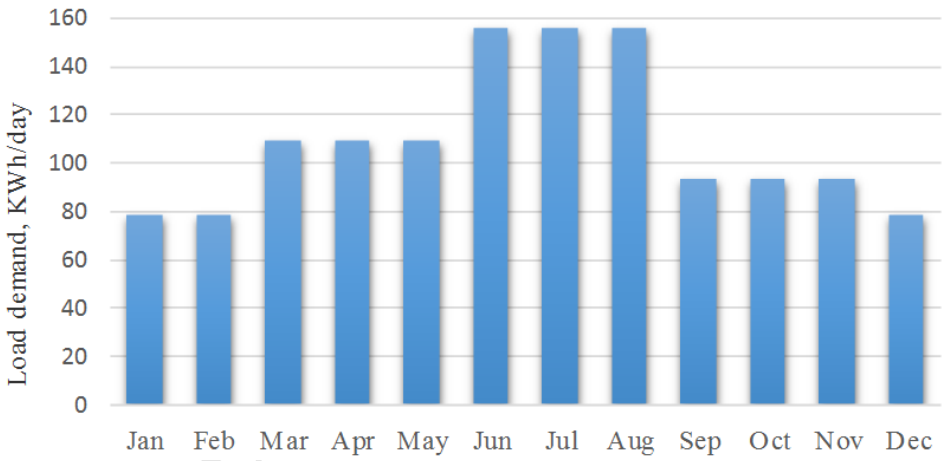

Fig. 2 BWP daily load demand for each month

As can be seen in the figure, the BWP is increased in summer compared to that in winter that inconsistency with the increase of the water in summer compared to that in winter as being discussed above. Due to its lower energy requirements, commercial RO units are shown in Table II that can treat water with <5,000 mg/L of dissolved solids (TDS) and <30 mg/L of suspended solids, is considered to achieve good water quality for the current case.

The standard treatment process involves pre-filtration (auto backwashing multimedia filters and cartridge filters), anti-scalant dosing to prevent membrane scaling, RO desalination and a cleaning-in-place system for membrane cleaning. Fig. 3 shows an overview of the proposed RO unit and Table II shows the specification of different RO units.

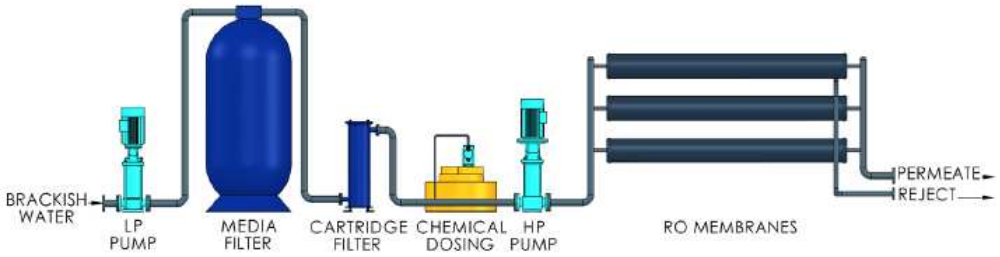

Fig. 3 Schematic diagram showing the main components of the proposed RO unit [52].

As 75 m^3 per day of treated water, i.e., permeate, is required, the RO-150 unit is selected to be used for the operation of 12 hours from 8 am to 18 pm. The required electrical energy for the RO unit is 126 kWh per day with 10.5 peak demand. Therefore, the total required energy for both the BWP and RO unit approximately 236 kWh per day.

Table II Standard specification of different RO units

parameter	units	RO-50	RO-100	RO-150	RO-250	RO-500	RO-1000
Permeate Flow Rate	m^3/day	50	100	150	250	500	1000
Permeate Recovery Rate	%	60~85					
Permeate TDS	Mg/L	<500 (typical)					
Raw water TDS	Mg/L	<5000					
Raw water TSS	Mg/L	<30					
Power supply		AC 380-450 V, 3 Phase, 50/60 Hz					
Power consumption	KW	4.1	7.7	10.5	15	29.5	52

Monthly mean daily solar radiation data were obtained for the site from NASA surface meteorology and solar energy database [53]. Using these available daily data, HOMER is used for calculating both the clearance index and the hourly solar radiation intensity using the latitude and longitude data of the selected site as shown in Fig. 4. As being seen in the figure, a maximum solar radiation intensity of 8.0 kWh/m^2/day could be attained in June, the smallest solar radiation intensity of 3.5 kWh/m^2/day is attained in December, and generally a well solar distribution with an average intensity of 5.97 kWh/m^2/day is available all over the year. Fig. 5 shows the hourly solar radiation of the selected site during the different months. As is clear from the figure, the site has a sunshine duration of around 9 h/ day. In general, the intensity of the sun radiation is increased in the noon time and the summer compared to those in winter and in general the value of the solar intensity and that sunshine duration are suitable for PV usage [5].

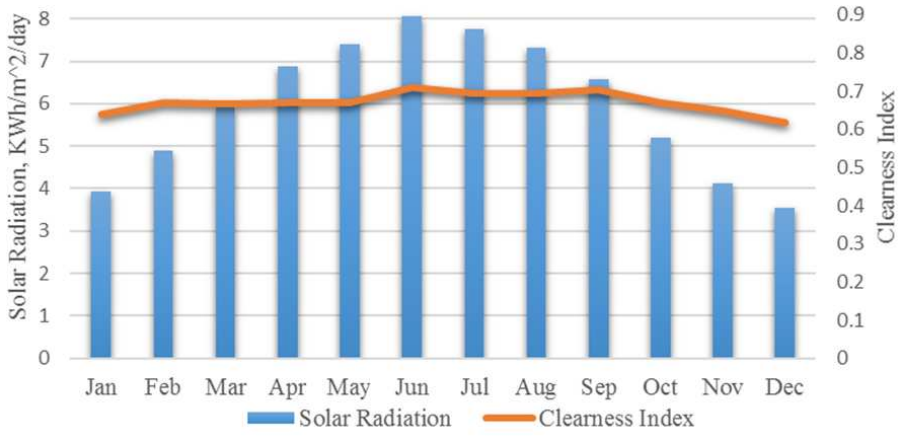

Fig. 4 Variation of solar radiation intensity and clearance index during each month

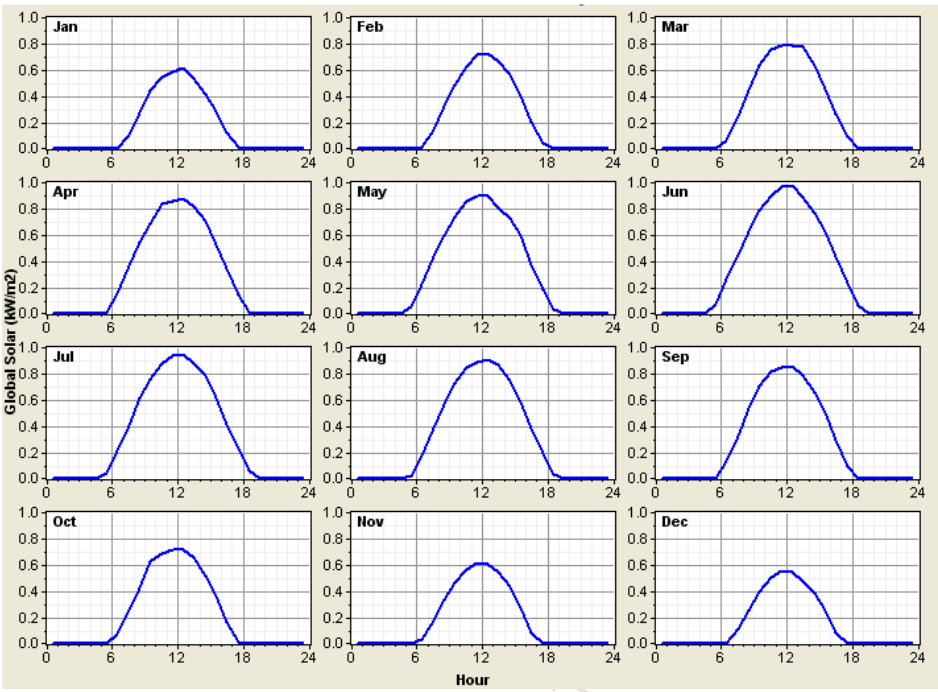

Fig. 5 Average hourly solar radiation distribution for each month (kW/m^2).

3. Configuration of the Proposed System

A schematic diagram of the proposed hybrid PV/SCFC-RO/BWP system is shown in Fig. 6 that consists of PV array, self-charging fuel cell, electrolyzer, power conditioning unit (PCU) and hydrogen storage tank. When PV is irradiated with the solar energy, it produces the energy that is required for operating the RO/BWP system, and the excess power is used in the electrolyzer for producing hydrogen that in turn stored in the hydrogen storage tank. At night and/or in case of low PV energy output due to the absence or decrease in the solar irradiance, hydrogen from the storage tank is used for producing energy in the FC to operate the RO/ BWP systems. A converter, i.e., PCU, is used to regulate between AC and DC. Table III shows the technical and economic specifications of the PV/SCFC RO/ BWP system components. A brief description of each component of the hybrid PV/SCFC-RO/ BWP is summarized in the following section.

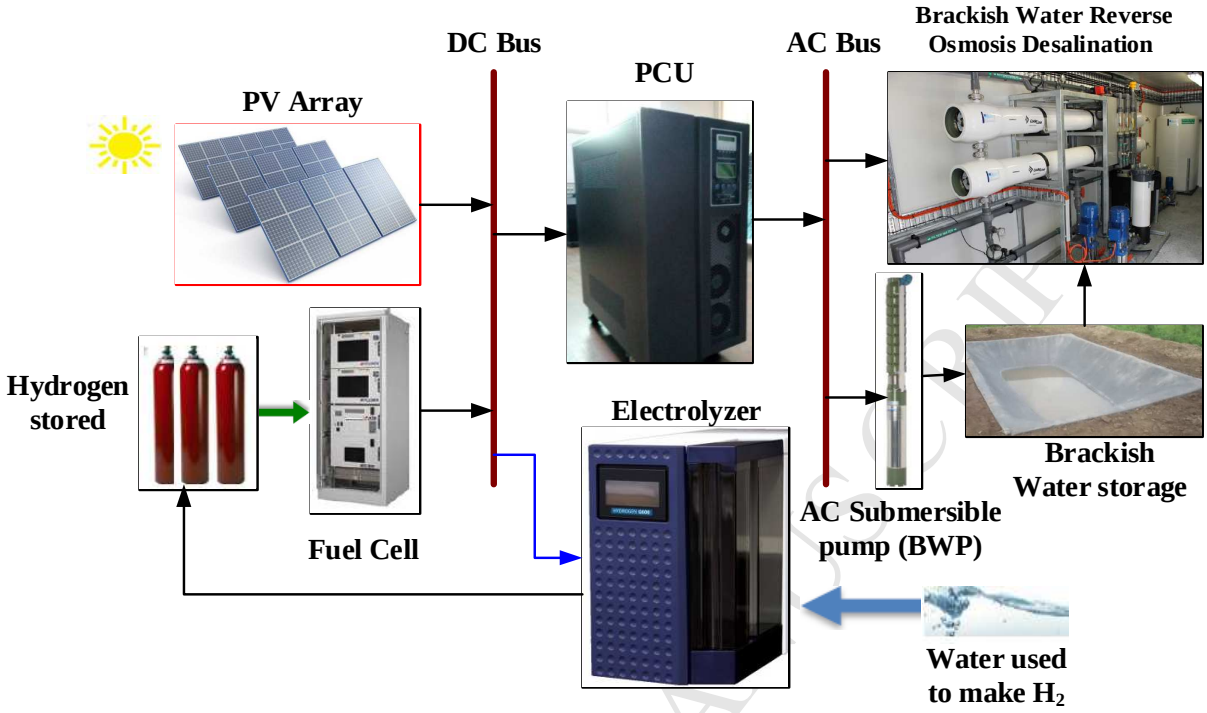

Fig. 6 Block diagram of PV/SCFC RO/ BWP system.

A. Solar PV panel selection

A proper PV panel for the proposed system is selected from fifteen different solar panels manufactured by different companies such as Ritek, Trina Solar, Conergy, EcoSolargy, SolarWorld, Sharp, Canadian Solar, Conergy, Yingli, Samsung, SolarWorld, Helios, CSUN and BenQ. The electrical and economical specifications for each type are shown in Table IV. The replacement cost is assumed to be the same as that of the initial PV panel cost. As PV panels require negligible operating and maintenance, the operating and maintenance costs were neglected. No tracking system is used. Therefore, the PV arrays are modeled to be fixed towards the south with an angle equal to the latitude angle; therefore, the sun will be perpendicular to the panel arrays for largest number of hours throughout the year, and maximum solar radiation could be received [50, 51]. Surrounding temperature is one of the main parameters that affect the solar PV power output where it decreased with increasing temperature according to the following equation [54]:

$$P_{pv} = f_{pv} \times Y_{pv} \times \frac{G_T}{G_S} \times \left\{1 + \alpha\left(T_c - T_{c,ref}\right)\right\} \quad (2)$$

Where;

P_{pv} energy produced from each PV module in kWh ;

Y_{pv} maximum power output of the PV module;

f_{pv} PV derating factor;

G_T global solar radiation intensity on the PV surface (kWh/m^2);

G_S standard solar radiation intensity,1 kW/m^2;

α temperature coefficient of power;
$T_{c,ref}$ Standard temperature of the PV module, 25$^{\circ}C$;
T_c temperature of the PV module in $^{\circ}C$;

PV power is significantly decreased with increasing temperature as seen from the temperature coefficient of power and the negative value that indicates the decrease in power with increasing temperature. α depends on the type of PV module and is usually provided by the manufacturer. When PV performance is not affected by temperature, α is negligibly small, and it is considered to be zero [39]. In the current study, the effect of temperature on PV performance was considered. Ground reflectance (albedo) which is defined as the fraction of radiation reflected by ground is another important factor that affects PV performance, and it will be considered to be 20 % in this study.

Table III. Techno-economical specifications for the different components of hybrid PV/SCFC system.

Component & Description	**Specification**
1. power conditioning unit [41, 55]	
rated power	1 kW
efficiency	90%
capital cost	400 $/kW
replacement cost	350 $/kW
maintenance cost	10 $/kW/year
lifetime	15 years
2. Fuel Cell [56]	
capital cost	3000 $/kW
replacement cost	2500 $/kW
maintenance cost	0.02 $/h
lifetime	40000 h
efficiency	90 %
3. Electrolyzer [56]	
capital cost	500 $/kW
replacement cost	250 $/kW
lifetime	$10/year
efficiency	85 %
4. Hydrogen Storage Tank	
capital cost	500 $/kW
replacement cost	250 $/kW
lifetime	10 $/year
efficiency	90 %

Table IV. Specification of different solar panels considered in the case study [57]

no	PV model	Manufacture	Origin country	Solar cell Type	No. of cells	power	Efficiency %	Voltage at MPP	Current at MPP	Tem. Coef.	NOCT	Price $
1	**PM230**	Ritek	Taiwan	Polycrystalline	60	230	14.05	29	7.89	-0.376	49.1	259
2	**TSM240PA05**	Trina	China	Polycrystalline	60	240	14.71	29.7	8.1	-0.43	45	240
3	**PM-240P**	Conergy	China	Polycrystalline	60	240	14.40	29.65	8.10	–0.44	46	230
4	**ECO240S156P-60**	EcoSolargy	China	Polycrystalline	60	240	14.76	30.3	7.91	-0.477	46	209
5	**SW-240 Poly**	SolarWorld	USA	Polycrystalline	60	240	14.61	30.2	7.96	-0.48	46	255
6	**ND-240QCJ**	Sharp	USA	Polycrystalline	60	240	14.70	29.3	8.19	-0.485	47.5	279
7	**CS6P-245M**	Canadian Solar	China	Mono-crystalline	60	245	15.23	30.3	8.09	-0.45	45	250
8	**PH-250P**	Conergy	China	Polycrystalline	60	250	15.20	30.30	8.27	–0.47	43	245
9	**YL250P-29b Poly**	Yingli	China	multicrystalline	60	250	15.30	30.4	8.24	-0.45	46	250
10	**PV-MBA1BG250**	Samsung	Korea	Mono-crystalline	60	250	15.33	30.7	8.15	-0.438	45	294
11	**SW-250 Mono**	SolarWorld	USA	Mono crystalline	60	250	14.91	37.1	8.05	-0.43	48	269
12	**6T-250**	Helios	USA	mono-crystalline	60	250	14.50	30.30	8.22	-0.44	45	339
13	**CSUN260M Mono**	CSUN	China	monocrystalline	60	260	16.02	30.8	8.44	-0.423	45	270
14	**PM250P00-260**	BenQ	Taiwan	multicrystalline	60	260	16.01	31.2	8.34	-0.44	46	290
15	**MM300T**	Ritek	Taiwan	Monocrystalline	72	300	15.39	35.4	8.42	-0.46	46.5	329

B. Power Conditioning Unit

The power output of the PV arrays is DC current while that required for the RO/BWP system is AC current. Therefore DC/AC inverter is used. $400/kW is the capital cost of the inverter while the replacement cost is considered to be little bit lower, i.e., $350/kW [58]. Both of the operational and maintenance costs of the inverter is assumed to be $10/year based on an inverter efficiency of 90% with a lifetime of 10 years [59]. Different converters sizes are considered during analysis using HOMER. The technical data of the converter is shown in Table III.

C. Fuel Cell

Proton exchange membrane fuel cells (PEMFCs) are effectively operating under different loads up to several hundred kWs and are available in commercial scale, are used in this study. PEMFCs use hydrogen as fuel and oxidant air (O_2) at the cathode where hydrogen is oxidized at anode producing protons and electrons, protons transported through the electrolyte membrane (Nafion) to the cathode side where they reacted with the electrons (transported in an external circuit to do the work) with oxygen from the surrounding air producing water as shown in the following equations:

At anode:

$$H_2 \rightarrow 2\,H^+ + 2\,e^{-1}$$

At cathode

$$2\,H^+ + 2\,e^{-1} + \frac{1}{2}O_2 \rightarrow H_2O$$

Overall reaction

$$H_2 + \frac{1}{2}O_2 \rightarrow H_2O$$

Due to the high efficiency, and no environmental impact, PEMFCs are considered as an effective way for storing renewable energy from wind and/or PV arrays where the excess energy from the PV and/or wind turbines is used for water electrolysis producing hydrogen that in turn used for electricity generation in the PEMFCs; therefore, it can be used for supplying energy in the time of low or no available energy from the PV panel . Compared to batteries, using the PEMFC as an energy storage device has several merits such as long lifetime, silent, and no environmental impact where water is the only byproduct.

The HOMER did a comparison between different powers of FCs based on Based on minimum NPC and COE that resulted in finding that an FC of 9 kW is considered. The economic specifications of the PEMFC are shown in Table III.

D. Electrolyzer

An electrolyzer is an electrochemical device that is used for converting electrical energy into chemical energy with high efficiency. It is usually used for generating hydrogen from water that in turn used for different applications such as fuel for PEMFC. The importance of electrolyzer is increased with increasing the usage of renewable energy where it was used as an effective tool for storing excess energy into hydrogen [60-62]. The electrolyzer as any electrochemical cell consists of two electrodes and an electrolyte. An electrolyzer of up to 15 kW is used in this study. The electrolyzer economic specifications are shown in Table III [56].

4. EVALUATION CRITERIA

A comparison between the different proposed configurations is carried out based on both total NPC and COE. NPC is calculated based on capital costs, O&M costs, including replacement costs for the proposed live time, and the salvage value that represents the value of the component at the end of the estimated lifetime of the system. The NPC was estimated based on the following equation [43]:

$$NPC = \frac{C_{total}}{CRF(i,t)} \quad (3)$$

Where;

t proposed lifetime of the project;

C_{total} The annual total cost of the proposed system ($/year);

i real annual interest rate (%);

CRF capital recovery factor.

The real annual interest rate considers the annual variation in the costs due to inflation compared with the on-time (current) cost of the system and it is estimated as follows:

$$i = \frac{i' - f}{1 + f}$$

Where;

i' Nominal interest rate;

f Annual inflation rate.

CRF is used to calculate the saving that has to be done to recover the initial price of the system during the proposed system cycle life using the following equation [63]:

$$CRF(i,n) = \frac{i(1+n)^n}{(1+n)^n - 1}$$, where n is the proposed system cycle life in years

In the case study, the cycle life is assumed to be 25 years

COE is simply the average cost of electrical energy unit (kWh) produced by the system, and it is calculated from the total annual costs of the system to the total energy produced during this year, as follows [63]:

$$COE = \frac{C_{ann,total}}{E_{total}} \quad (4)$$

Where;

E_{total} annual energy production rate (kWh/year);

$C_{ann,total}$ total costs of the system during the year.

The annual total cost of the system includes all types of expenses such as annual operating and maintenance costs, annualized capital, recovery, and replacement costs.

5. SIMULATION RESULTS AND DISCUSSIONS

Table V and Fig. 7 show the COE and NPC for each type of solar panel. From this figure, it can be concluded that the optimum configuration reached with employing ECO240S156P-60 solar panel manufactured by EcoSolargy. This configuration includes PV array (66 kW), FC (9 kW), converter (25 KW) –Electrolyzer (15 kW), Hydrogen tank (25 kg) shows the best economic viable option based on the NPC and COE values of $71,806 and $0.047; respectively. The effect of the PV/SCFC size on the various costs is shown in Table VI.

Table V Optimum size of PV/SCFC hybrid system under different types of solar panels

no	PV model	PV (KW)	FC(KW)	Conv.(KW)	Elec.(KW)	H_2 Tank (kg)	Initial cost($)	Operating Cost ($)	Capital cost, $	COE $/kWh
1	**PM230**	67	9	25	14	60	119,502	580	132,278	0.071
2	**TSM240PA05**	67	9	25	14	60	111,060	581	123,865	0.066
3	**PM-240P**	66	9	25	15	65	107,859	614	121,387	0.065
4	**ECO240S156P-60**	66	9	25	15	70	101,990	620	115,649	0.062
5	**SW-240 Poly**	66	9	25	15	70	114,728	620	128,387	0.069
6	**ND-240QCJ**	66	9	25	15	70	121,328	622	135,017	0.072
7	**CS6P-245M**	66	9	25	15	65	111,885	614	125,398	0.067
8	**PH-250P**	66	9	25	15	65	109,245	614	122,773	0.066
9	**YL250P-29b Poly**	66	9	25	15	65	110,565	616	124,138	0.066
10	**PV-MBA1BG250**	66	9	25	15	65	114,261	614	127,789	0.068
11	**SW-250 Mono**	66	9	25	15	65	115,576	604	128,884	0.069
12	**6T-250**	66	9	25	18	95	130,167	728	146,211	0.078
13	**CSUN260M Mono**	63	9	25	17	85	111,042	694	126,322	0.068
14	**PM250P00-260**	63	9	25	17	90	115,898	697	131,248	0.07
15	**MM300T**	66	9	25	15	70	116,972	621	130,646	0.07

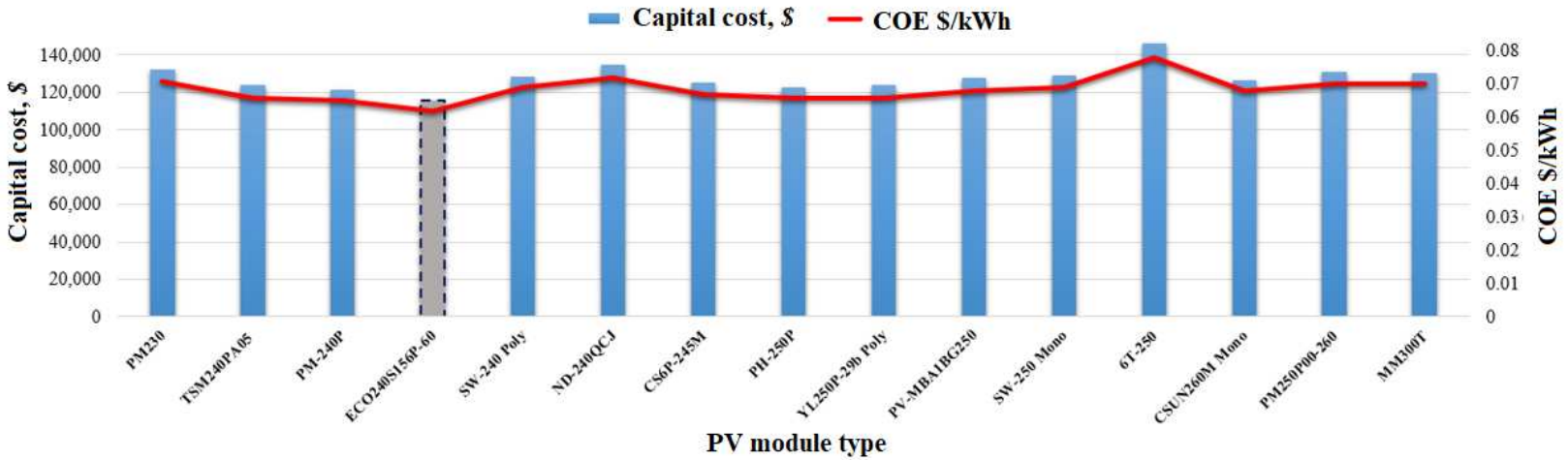

Fig. 7 COE and NPC using different types of solar modules

Table VI. Different costs associated with the optimal size of PV/SCFC

Component	Optimum size	Capital ($)	Replacement ($)	O&M ($)	Salvage ($)	Total ($)
PV	66 kW	57,420	0	0	0	57,420
FC	9 kW	27,000	0	5,736	-1,678	31,058
PCU	25 kW	10,000	7,537	0	-2,274	15,262
electrolyzer	15 kW	7,500	3,303	330	-2193	11,684
H_2 tank	70 kg	70	0	154	0	224
PV/FC system		101,990	10,610	9,194	-6,145	115,649

Fig. 8 shows a cash flow break-down of the main components of the system. The capital cost is found to be $101,990 while total NPC is $115,649. The corresponding annual COE and annual operating costs are 0.062 $/kWh and $ 620, respectively. The cost of the 66 kW PV array represents 56.30 % of the total NPC, FC cost represents 26.47 %, and other components represent less than 10 %. Total annual energy of 144,082 kWh is expected using PV/SCFC. The sharing rates for PV array and FC are 92 % (132,285 kWh/year) and 8 % (11,797 kWh/year) respectively. The monthly mean electric production from PV array and FC is presented in Fig. 9. Fig. 10 displays the daily rate of hydrogen production (based on the excess energy produced from the PV system after providing the energy required for the RO/BPW system) throughout the different months in the year. A total hydrogen production of 715 kg/year is expected with a cost of 7.53 $/kg. The annual energy consumption rates are 38% (45,232 KWh/), 34 % (39,695 KWh) and 28 % (33,159 KWh) for RO unit, BWP unit and electrolyzer respectively. It can be seen that major part of the power required for the site is supplied directly by the PV while an average of 10 % of the total power was secured by the FC system from lowest percentage of 7 % in May to 14% in July. Although it was expected that the rely in the FC will increase in winter where lower solar irradiance intensity and duration, the results showed a decrease in relying on FC in winter compared to that in summer, and this would be related to the increased power requirements in the summer as can be seen for BWP shown in Fig. 2. In general, the power from the PV and that stored by the electrolyzer/FC system is adequate for supplying the total power requirements of the site. Moreover, there is some extra energy available from the electrolyzer/FC that will be used for other small power requirements such as powering small pumps used for the distribution of the water in the land.

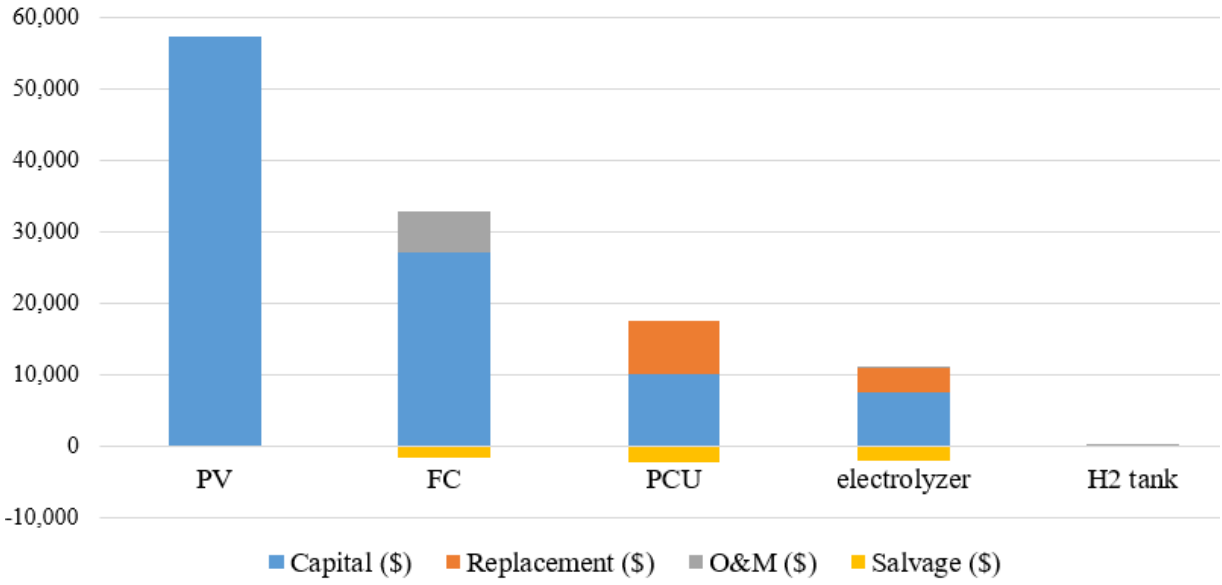

Fig. 8 Cash flow break-down of the different components PV/SCFC

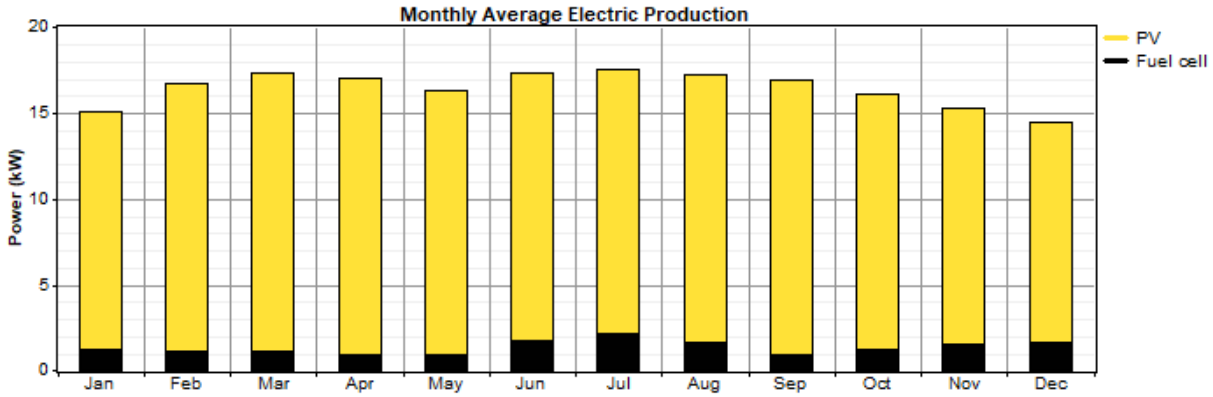

Fig. 9 Monthly average electric production of PV/SCFC system

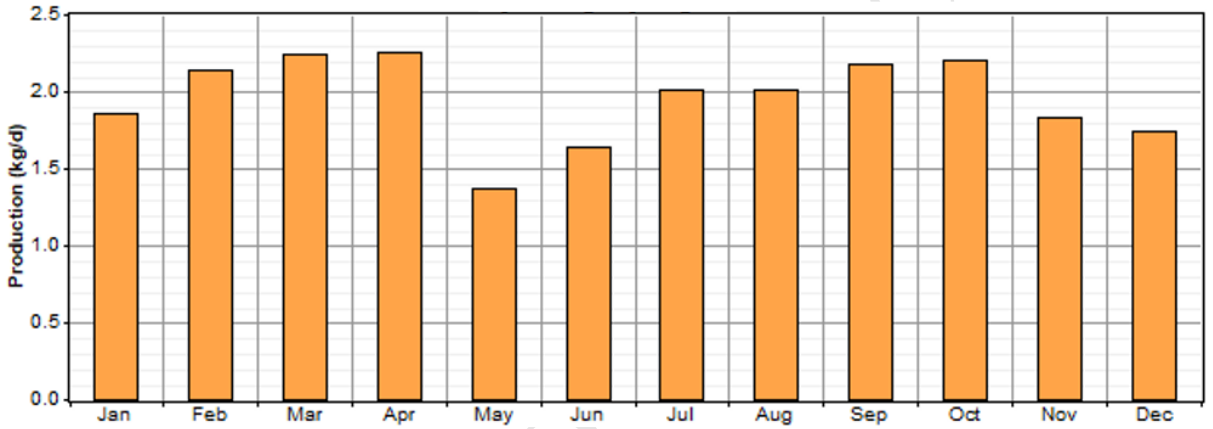

Fig. 10 Daily hydrogen production for each month

6. COMPARISON STUDY

From the above section, it was clear that applying the optimized PV/SCFC is a cost-effective and effectively used for maintaining power supply for the system without any intermittence. However, comparing this system with traditional ways is important. In this section, we will make a techno-economical comparison of the PV/SCFC system with a stand-alone diesel generation system as well as with grid extension based on the total NPC and COE.

6.1 Stand-alone Diesel Generation System

The fuel consumption, F_G (L/h), in the diesel generation system is calculated based on the of the power output as follows [22];

$$F_G = B_G \times P_{G-rated} + A_G \times P_{G-out} \quad (5)$$

Where $P_{G-rated}$ is the nominal power

P_{G-out} is the output power

A_G and B_G denote the coefficients of fuel consumption curve (L/KWh)

The replacement and capital cost of the DG are considered to be \$230/kW of each while operational costs are assumed to be \$0.1/h based on an operation life time of 15,000 h [58]. The current price of diesel in Egypt is \$0.2/l that is significantly subsided. However this price can be doubled in the arid areas due to the high transportation cost. The simulation results indicated that the optimum size of the DG is 18 kW based on the official diesel price of 0.2

$/l; however this can increase using the actual price of diesel in the arid areas. Therefore 0.002 $/km distance from the nearest gasoline station is added to the official diesel price. The simulation results based on the 0.23 $/l shows an initial cost and a total NPC of $4,140 and $391,690 respectively. The corresponding annual COE and operating costs are 0.206 $/kWh and $17,597 respectively. Fig. 11 shows the effect of diesel price on both COE and total NPC. As is clear from the figure, both of the total NPC and COE are significantly increased with increasing diesel price where COE changed from $0.206/kWh to $ 0.576/kWh, and NPC changed from $ 391,690 to $ 1,093,493 with the increase of diesel price from 0.23 $/L to 1.2 $/L.

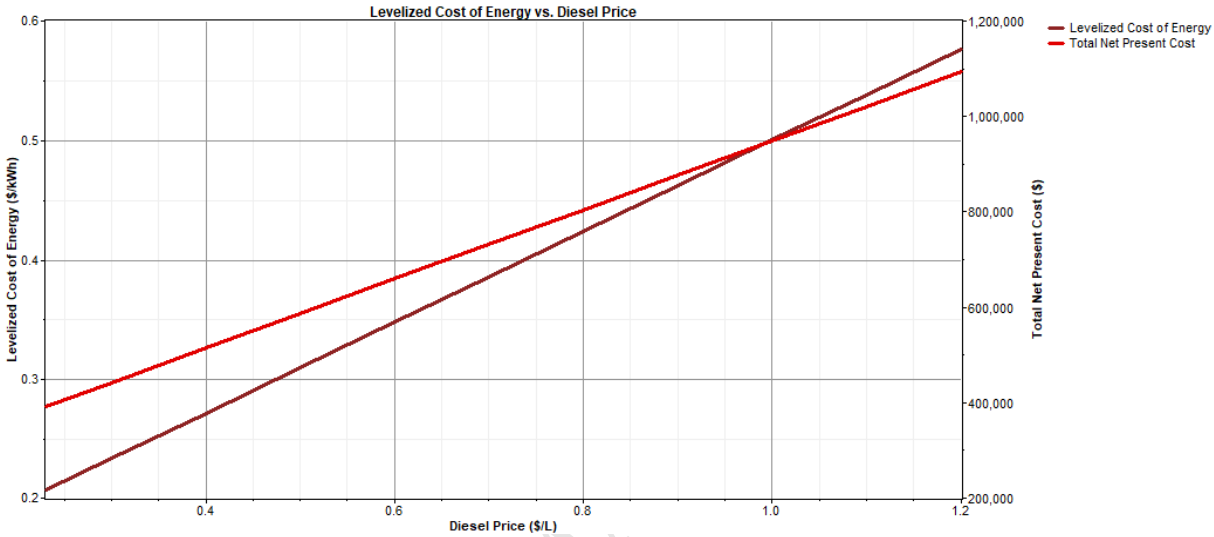

Fig. 11 Effect of diesel price on COE and NPC

6.2 Grid Extension

The other option that will be used for comparison with the proposed PV/SCFC hybrid system is a cost analysis of the grid extension to the desired arid area which will be used as standard benchmark. In this study, the grid extension is proposed as a pure radial line. Based on the current prices in Egypt, the capital cost and the annual O&M cost are taken as $5,000/km and $150/year/km, respectively. A 0.025 $/kWh is the latest grid energy cost issued by Egyptian electricity ministry [64]. The effect of the grid extension distance on NPC of the three proposed systems, i.e., PV/SCFC, stand-alone DG, and grid extension, is shown in Fig. 12. As seen from the figure, the grid is more economical at a short distance up to 41.5 km and 8.21 km in case of DG and PV/SCFC, respectively, while at longer distances it is a no longer viable option.

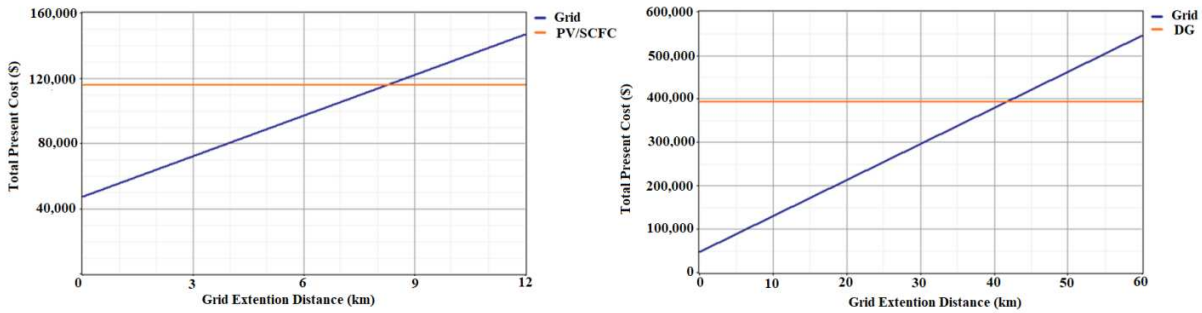

Fig. 12 Breakeven grid extension distance for DG system and PV/SCFC hybrid system

7. Environmental effects

Due to global warming, a general intention is paid now for controlling the pollution by relying on the renewable energy sources that have no environmental impacts compared with those relies on fossil fuels. Table VII shows the quantity of different pollutants emissions optimum PV/SCFC hybrid renewable system compared with the stand-alone DG system. The DG system produces 86,500 kg/year of CO_2 in the site. This amount can be removed by using PV/SCFC hybrid renewable system. Other pollutants also reduced compared to the DG system. Therefore, in addition to the PV/SCFC hybrid system configuration being a more economically viable option, the system also can help to abate prevalent global warming, which usually occurred as a result of CO_2 emission into the environment.

Table VII Pollutants emission in the case of PV/SCFC hybrid system and DG system

Pollutant	**Emission** (kg/year)	
	stand-alone DG system	PV/SCFC hybrid system
Carbon dioxide	86,511	0.00
Carbon monoxide	214	0.00
Unburned hydrocarbons	23.7	0.00
Particulate matter	16.1	0.00
Sulfur dioxide	174	0.00
Nitrogen oxides	1,905	0.00

8. CONCLUSIONS

This paper investigated the use of fuel cell as storage in a stand-alone hybrid system for supplying electrical energy to brackish water pumping and reverse osmosis (BWP/RO) desalination system. The minimum total NPC and the COE were used to determine the optimum system sizing. In the case study, the optimization results indicated that the PV/FC system performed the best choice compared with the diesel generation system in both minimum COE and NPC. Considering the grid extension, PV/SCFC BWP/RO desalination system was more economically viable than grid extension. Findings indicated that the PV array (66 kW), FC (9 kW), converter (25 KW) –Electrolyzer (15 kW), Hydrogen tank (70 kg) was the most economically viable option with the total net present cost of $115,649 and per unit cost of electricity of $0.062.

Additionally, a comparison with stand-alone diesel generation (DG) system and with grid extension was carried out against the optimal configuration of PV/SCFC HRES. The COE for the stand-alone DG system is 0.198 $/kWh which was 76.26 % higher than that of the PV/SCFC system. The breakeven grid extension distance for DG system and PV/SCFC hybrid system were 41.5 km and 8.21 km respectively. The avoided CO_2 emissions by displacing diesel fuel would be 70,974 kg/year for the PV/SCFC Powered brackish BWP and RO desalination plant. FCs demonstrated a practical storage solution for photovoltaics from the economic and environmental point of views.

9. Acknowledgments

This work was supported by the University of Sharjah, Project No. 18020406122.

10. REFERENCES

[1] Ben Ali I, Turki M, Belhadj J, Roboam X. Optimized fuzzy rule-based energy management for a battery-less PV/wind-BWRO desalination system. Energy. 2018;159:216-28.

[2] Abdelkareem MA, El Haj Assad M, Sayed ET, Soudan B. Recent progress in the use of renewable energy sources to power water desalination plants. Desalination. 2018;435:97-113.

[3] Ma W, Xue X, Liu G. Techno-economic evaluation for hybrid renewable energy system: Application and merits. Energy. 2018;159:385-409.

[4] Klingler A-L. The effect of electric vehicles and heat pumps on the market potential of PV + battery systems. Energy. 2018;161:1064-73.

[5] Ooi JB, Ismail HM, Tan BT, Wang X. Effects of graphite oxide and single-walled carbon nanotubes as diesel additives on the performance, combustion, and emission characteristics of a light-duty diesel engine. Energy. 2018;161:70-80.
[6] Vijay A, Hawkes A. Impact of dynamic aspects on economics of fuel cell based micro co-generation in low carbon futures. Energy. 2018;155:874-86.
[7] Abdelkareem MA, Allagui A, Sayed ET, El Haj Assad M, Said Z, Elsaid K. Comparative analysis of liquid versus vapor-feed passive direct methanol fuel cells. Renewable Energy. 2019;131:563-84.
[8] Barakat NAM, Moustafa HM, Nassar MM, Abdelkareem MA, Mahmoud MS, Almajid AA, et al. Distinct influence for carbon nano-morphology on the activity and optimum metal loading of Ni/C composite used for ethanol oxidation. Electrochimica Acta. 2015;182:143-55.
[9] Barakat NAM, Abdelkareem MA, Shin G, Kim HY. Pd-doped Co nanofibers immobilized on a chemically stable metallic bipolar plate as novel strategy for direct formic acid fuel cells. International Journal of Hydrogen Energy. 2013;38(18):7438-47.
[10] Badur J, Lemański M, Kowalczyk T, Ziółkowski P, Kornet S. Zero-dimensional robust model of an SOFC with internal reforming for hybrid energy cycles. Energy. 2018;158:128-38.
[11] Abdelkareem MA, Tanveer WH, Sayed ET, Assad MEH, Allagui A, Cha SW. On the technical challenges affecting the performance of direct internal reforming biogas solid oxide fuel cells. Renewable and Sustainable Energy Reviews. 2019;101:361-75.
[12] Sharma S, Celebi AD, Maréchal F. Robust multi-objective optimization of gasifier and solid oxide fuel cell plant for electricity production using wood. Energy. 2017;137:811-22.
[13] Cai W, Liu J, Liu P, Liu Z, Xu H, Chen B, et al. A direct carbon solid oxide fuel cell fueled with char from wheat straw. International Journal of Energy Research. 2018.
[14] Abdelkareem MA, Al Haj Y, Alajami M, Alawadhi H, Barakat NAM. Ni-Cd carbon nanofibers as an effective catalyst for urea fuel cell. Journal of Environmental Chemical Engineering. 2018;6(1):332-7.
[15] Sayed ET. Yeast Extract as an Effective and Safe Mediator for the Baker's-Yeast-Based Microbial Fuel Cell. Industrial & engineering chemistry research.54(12):3116-22.
[16] Mohamed HO, Abdelkareem MA, Obaid M, Chae S-H, Park M, Kim HY, et al. Cobalt oxides-sheathed cobalt nano flakes to improve surface properties of carbonaceous electrodes utilized in microbial fuel cells. Chemical Engineering Journal. 2017;326:497-506.
[17] Sun H, Yu M, Li Q, Zhuang K, Li J, Almheiri S, et al. Characteristics of charge/discharge and alternating current impedance in all-vanadium redox flow batteries. Energy. 2019;168:693-701.
[18] Weng G-M, Li C-YV, Chan K-Y. Three-electrolyte electrochemical energy storage systems using both anion- and cation-exchange membranes as separators. Energy. 2019;167:1011-8.
[19] Weng G-M, Vanessa Li C-Y, Chan K-Y. Hydrogen battery using neutralization energy. Nano Energy. 2018;53:240-4.
[20] Weng G-M, Li C-YV, Chan K-Y. High-voltage pH differential vanadium-hydrogen flow battery. Materials Today Energy. 2018;10:126-31.
[21] Huskinson B, Marshak MP, Suh C, Er S, Gerhardt MR, Galvin CJ, et al. A metal-free organic–inorganic aqueous flow battery. Nature. 2014;505:195.
[22] Zhang X, Chan SH, Ho HK, Tan S-C, Li M, Li G, et al. Towards a smart energy network: The roles of fuel/electrolysis cells and technological perspectives. International Journal of Hydrogen Energy. 2015;40(21):6866-919.
[23] Ehteshami SMM, Chan SH. The role of hydrogen and fuel cells to store renewable energy in the future energy network – potentials and challenges. Energy Policy. 2014;73:103-9.
[24] Shabani B, Andrews J, Watkins S. Energy and cost analysis of a solar-hydrogen combined heat and power system for remote power supply using a computer simulation. Solar Energy. 2010;84(1):144-55.

[25] Ameri M, Yoosefi M. Power and Fresh Water Production by Solar Energy, Fuel Cell, and Reverse Osmosis Desalination. 2016.
[26] Smaoui M, Abdelkafi A, Krichen L. Optimal sizing of stand-alone photovoltaic/wind/hydrogen hybrid system supplying a desalination unit. Solar Energy. 2015;120:263-76.
[27] Touati S, Belkaid A, Benabid R, Halbaoui K, Chelali M. Pre-feasibility design and simulation of hybrid pv/fuel cell energy system for application to desalination plants loads. Procedia engineering. 2012;33:366-76.
[28] Ghenai C, Bettayeb M. Modelling and performance analysis of a stand-alone hybrid solar PV/Fuel Cell/Diesel Generator power system for university building. Energy. 2019;171:180-9.
[29] Luta DN, Raji AK. Optimal sizing of hybrid fuel cell-supercapacitor storage system for off-grid renewable applications. Energy. 2019;166:530-40.
[30] Das BK, Zaman F. Performance analysis of a PV/Diesel hybrid system for a remote area in Bangladesh: Effects of dispatch strategies, batteries, and generator selection. Energy. 2019;169:263-76.
[31] Fodhil F, Hamidat A, Nadjemi O. Potential, optimization and sensitivity analysis of photovoltaic-diesel-battery hybrid energy system for rural electrification in Algeria. Energy. 2019;169:613-24.
[32] Ghenai C, Merabet A, Salameh T, Pigem EC. Grid-tied and stand-alone hybrid solar power system for desalination plant. Desalination. 2018;435:172-80.
[33] Ghenai C, Salameh T, Merabet A. Technico-economic analysis of off grid solar PV/Fuel cell energy system for residential community in desert region. International Journal of Hydrogen Energy. 2018.
[34] Singh A, Baredar P, Gupta B. Techno-economic feasibility analysis of hydrogen fuel cell and solar photovoltaic hybrid renewable energy system for academic research building. Energy Conversion and Management. 2017;145:398-414.
[35] Rajbongshi R, Borgohain D, Mahapatra S. Optimization of PV-biomass-diesel and grid base hybrid energy systems for rural electrification by using HOMER. Energy. 2017;126:461-74.
[36] Margaret Amutha W, Rajini V. Techno-economic evaluation of various hybrid power systems for rural telecom. Renewable and Sustainable Energy Reviews. 2015;43:553-61.
[37] Khan MRB, Jidin R, Pasupuleti J, Shaaya SA. Optimal combination of solar, wind, micro-hydro and diesel systems based on actual seasonal load profiles for a resort island in the South China Sea. Energy. 2015;82:80-97.
[38] Lau K, Tan C, Yatim A. Photovoltaic systems for Malaysian islands: Effects of interest rates, diesel prices and load sizes. Energy. 2015;83:204-16.
[39] Rohani G, Nour M. Techno-economical analysis of stand-alone hybrid renewable power system for Ras Musherib in United Arab Emirates. Energy. 2014;64:828-41.
[40] Kusakana K. Techno-economic analysis of off-grid hydrokinetic-based hybrid energy systems for onshore/remote area in South Africa. Energy. 2014;68:947-57.
[41] Li C, Ge X, Zheng Y, Xu C, Ren Y, Song C, et al. Techno-economic feasibility study of autonomous hybrid wind/PV/battery power system for a household in Urumqi, China. Energy. 2013;55:263-72.
[42] Mohammed M, Aziz A, Alwaeli AH, Kazem HA. Optimal sizing of photovoltaic systems using HOMER for Sohar, Oman. International Journal of Renewable Energy Research (IJRER). 2013;3(3):470-5.
[43] Hiendro A, Kurnianto R, Rajagukguk M, Simanjuntak YM. Techno-economic analysis of photovoltaic/wind hybrid system for onshore/remote area in Indonesia. Energy. 2013;59:652-7.
[44] Hiendro A, Kurnianto R, Rajagukguk M, Simanjuntak YM, Junaidi. Techno-economic analysis of photovoltaic/wind hybrid system for onshore/remote area in Indonesia. Energy. 2013;59:652-7.
[45] Nandi SK, Ghosh HR. Prospect of wind–PV-battery hybrid power system as an alternative to grid extension in Bangladesh. Energy. 2010;35(7):3040-7.
[46] Rehman S, Al-Hadhrami LM. Study of a solar PV–diesel–battery hybrid power system for a remotely located population near Rafha, Saudi Arabia. Energy. 2010;35(12):4986-95.

[47] Lau KY, Yousof M, Arshad S, Anwari M, Yatim A. Performance analysis of hybrid photovoltaic/diesel energy system under Malaysian conditions. Energy. 2010;35(8):3245-55.
[48] Rezk H, El-Sayed AHM. Sizing of a stand alone concentrated photovoltaic system in Egyptian site. International Journal of Electrical Power & Energy Systems. 2013;45(1):325-30.
[49] Rezk H, Shoyama M. Techno-economic optimum sizing of stand-alone photovoltaic/fuel cell renewable system for irrigation water pumping applications. Conference Techno-economic optimum sizing of stand-alone photovoltaic/fuel cell renewable system for irrigation water pumping applications. IEEE, p. 182-6.
[50] Rezk H, Dousoky GM. Technical and economic analysis of different configurations of stand-alone hybrid renewable power systems–A case study. Renewable and Sustainable Energy Reviews. 2016;62:941-53.
[51] Rezk H. A comprehensive sizing methodology for stand-alone battery-less photovoltaic water pumping system under the Egyptian climate. Cogent Engineering. 2016;3(1):1242110.
[52] RO company.
[53] NASA. Surface meteorology and energy. 2013.
[54] Wahidin S, Idris A, Shaleh SRM. Rapid biodiesel production using wet microalgae via microwave irradiation. Energy conversion and management. 2014;84:227-33.
[55] Vermaak HJ, Kusakana K. Design of a photovoltaic–wind charging station for small electric Tuk–tuk in DR Congo. Renewable energy. 2014;67:40-5.
[56] Silva S, Severino M, De Oliveira M. A stand-alone hybrid photovoltaic, fuel cell and battery system: A case study of Tocantins, Brazil. Renewable energy. 2013;57:384-9.
[57] Human G, van Schoor G, Uren KR. Power management and sizing optimisation of renewable energy hydrogen production systems. Sustainable Energy Technologies and Assessments. 2019;31:155-66.
[58] Olatomiwa L, Mekhilef S, Huda A, Sanusi K. Techno‐economic analysis of hybrid PV‐diesel‐battery and PV‐wind‐diesel‐battery power systems for mobile BTS: the way forward for rural development. Energy Science & Engineering. 2015;3(4):271-85.
[59] Asrari A, Ghasemi A, Javidi MH. Economic evaluation of hybrid renewable energy systems for rural electrification in Iran—A case study. Renewable and Sustainable Energy Reviews. 2012;16(5):3123-30.
[60] Shiroudi A, Taklimi SRH, Mousavifar SA, Taghipour P. Stand-alone PV-hydrogen energy system in Taleghan-Iran using HOMER software: optimization and techno-economic analysis. Environment, development and sustainability. 2013;15(5):1389-402.
[61] Arsalis A, Alexandrou AN, Georghiou GE. Thermoeconomic modeling of a completely autonomous, zero-emission photovoltaic system with hydrogen storage for residential applications. Renewable Energy. 2018;126:354-69.
[62] Bernal-Agustín JL, Dufo-López R. Techno-economical optimization of the production of hydrogen from PV-Wind systems connected to the electrical grid. Renewable Energy. 2010;35(4):747-58.
[63] Nema P, Nema R, Rangnekar S. Minimization of green house gases emission by using hybrid energy system for telephony base station site application. Renewable and Sustainable Energy Reviews. 2010;14(6):1635-9.
[64] Villanueva-Estrada RE, Rocha-Miller R, Arvizu-Fernández JL, Castro González A. Energy production from biogas in a closed landfill: A case study of Prados de la Montaña, Mexico City. Sustainable Energy Technologies and Assessments. 2019;31:236-44.

Highlights

1. Standalone hybrid photovoltaic and self-charging fuel cell (PV/SCFC) is proposed for RO.
2. Optimal PV/SCFC is better than diesel generation (DG).
3. COE and NPC are the lowest in PV/FC system compared to those in DG system.
4. PV/SCFC BWP/RO system is economical viable than grid extension up to 8.21 km.
5. DG is economical viable than grid extension up to 41.5 km.